Materials Science and Engineering C xxx (2009) xxx–xxx

Contents lists available at ScienceDirect

Materials Science and Engineering C

journal homepage: www.elsevier.com/locate/msec

Boronic acid functionalized superparamagnetic iron oxide nanoparticle as a novel tool for adsorption of sugar

S. Mohapatra [a,*], N. Panda [a], P. Pramanik [b]

[a] Department of Chemistry, National Institute of Technology, Rourkela-769008, India
[b] Department of Chemistry, Indian Institute of Technology, Kharagpur-721302, India

ARTICLE INFO

Article history:
Received 5 February 2009
Received in revised form 9 May 2009
Accepted 18 May 2009
Available online xxxx

Keywords:
Superparamagnetic
Nanoparticles
Magnetic separation
Boronic acid
Sugar binding

ABSTRACT

Synthesis of boronic acid functionalized superparamagnetic iron oxide nanoparticles has been reported. Magnetite nanoparticles were prepared by simple co-precipitation from Fe^{2+} and Fe^{3+} solution. *m*-Aminophenyl boronic acid was attached to iron oxide particles through 3,4-dihydroxy benzaldehyde through C=N bond. X-ray diffraction and selected area electron diffraction have shown the formation of inverse spinel phase magnetite of both as prepared and functionalized magnetite particles. FTIR shows attachment of boronic acid-imine onto iron oxide surface through enediol group. Transmission electron microscopy shows well dispersion of boronic acid functionalized particles of size 8 ± 2 nm. Vibration sample magnetometry shows both the particles are superparamagnetic at room temperature having saturation magnetization (Ms) 52 emu/g. In this work the affinity of these boronic acid functionalized particles towards sugar binding was studied taking dextrose sugar as a model. The influence of pH and sugar concentration has been extensively investigated. The results show that such boronic acid modified superparamagnetic particles are efficient support for sugar separation having maximum sugar loading capacity (60 μg/50 μl) at pH 8.

1. Introduction

The molecular recognition of sugars is an intriguing subject in view of its important role in detection/isolation of glycoconjugates such as glycoproteins and glycolipids [1]. Boronate affinity chromatography has been proved as a promising method to purify glycoproteins from a long time [2–5]. Based on the unique property of boronate ligand to reversibly form cyclic esters producing a five or six member ring with a 1, 2 diol in cis-coplanar geometry or a 1, 3 diol of proper geometry [6–8], boronate affinity chromatography has been frequently used as an ideal general extraction module for glycoconjugates [9]. The complexations of arylboronic acids with 1, 2-diols and 1, 3-diols have been largely used in separation [6], transport [10,11], and detection of sugars [12,13]. Thus for practical applications it is important to immobilize aryl boronic acid on insoluble solid supports in order to promote solid phase separation and reusability of aryl boronic acids. Conventionally, boronic acid carrying agarose or acrylamide-based polymeric beads have been used in chromatographic studies involving separation [14–18]. Recently Shimomura et al. have synthesized a solid magnetic support by modifying magnetite particles with graft polymerization of acrylic acid [19,20]. They have immobilized dihydroxyphenylboronic acid (DHPB) on modified magnetite surface through amide linkages and exploited the binding nature of various oligosaccharides with these boronic acid functionalized particles. However, these polymer or magnetic polymer based supports suffer from severe drawbacks owing to its less surface area which ultimately results in less binding efficiency. Development of a simpler and more versatile system for purification of sugars and sugar containing biomolecules has always been of great interest in this field.

In recent years, magnetic nanoparticles have been emerged as a new type of matrices for immobilization of proteins and enzymes [21–23]. We have designed surface modified magnetite nanoparticles for separation of histidine-tagged recombinant protein through immobilized metal ion chelate affinity chromatography [24]. Magnetic nanoparticles perform better than polymer macro-beads owing to its high surface-to-volume ratio resulting in high binding rate. More specifically, superparamagnetic iron oxide particles in nano regime are extensively used in bioseparation for their well-established biocompatibility [25]. In addition, due to superparamagnetism of inorganic cores, recovery and further usage of these solid supports can be facilely achieved by applying external magnetic field. Though the use of iron oxide nanoparticles have been extensively studied for immobilization and purification of proteins, surprisingly there has not yet been single report on design of such magnetic nanoparticles for isolation/purification of sugars. In this paper we have reported our preliminary study on synthesis of superparamagnetic magnetite nanoparticles with surface active boronic acid groups which can be used as a binder and carrier for sugars.

* Corresponding author.
E-mail address: sasmita05@gmail.com (S. Mohapatra).

0928-4931/$ – see front matter © 2009 Elsevier B.V. All rights reserved.
doi:10.1016/j.msec.2009.05.017

2. Experimental

2.1. Chemicals

All chemicals used here are of reagent grade and were used without further purification. $FeCl_3$ and $FeSO_4$ were obtained from Merck, Germany. *m*-Aminophenyl boronic acid was supplied from Sigma-Aldrich, USA and 3,4 dihydroxy benzaldehyde was obtained from Spectrochem, Mumbai, India.

2.2. Preparation of boronic acid functionalized superparamagnetic iron oxide nanoparticles

The synthetic strategy for these surface functionalized magnetic nanoparticles and the subsequent sugar binding mechanism has been outlined in Scheme 1. Boronic acid has been successfully attached to the surface of the magnetite nanoparticle through 3, 4 dihydroxy benzaldehyde. We have studied the sugar adsorption capacity of these boronic acid modified magnetite nanoparticles taking dextrose sugar as a model molecule.

2.2.1. Synthesis of boronic acid imine (1)

An equimolar amount of 3, 4 dihydroxybenzaldehyde was added to a solution of 3-aminophenyl boronic acid in absolutely dry methanol (0·36 mmol in 10 ml). The mixture was refluxed for 3 h during which a yellow solid was formed. The solid so formed was collected by filtration and recrystallised from methanol, M. P. 156 °C and characterized by FTIR, ^{1}H NMR, and MS. ^{1}H NMR (DMSO-d_6): δ 8.35 (s, 1H), 6.81–7.60 (m, 7H), 2.3 (s, 2H). IR (KBr) 2926, 2856, 1640 (C=N), 1596, 1504, 1330, 1228, 1106, 1036, 972, 860, 706 cm^{-1}, MS (ESI) m/z (relative intensity): 258.04 ($[M+H]^+$, 100).

2.2.2. Preparation of boronic acid functionalized iron oxide nanoparticles (2)

Superparamagnetic iron oxide nanoparticles were prepared according to our previously reported procedure [24]. In a typical recipe, 0.324 g $FeCl_3$ and 0.274 g $FeSO_4 \cdot 6H_2O$ were taken in 40 ml deionized water under argon atmosphere. 5 ml 25% NH_3 was injected into it while stirring at 4000 rpm in a mechanical stirrer under continuous argon flow for 1 h. 2.4 ml of this black colloidal suspension was withdrawn and the particles are separated and washed with 5 ml deionized water (5×1 ml) using a magnetic separator. Then the particles were sonicated in 5 ml absolutely dry DMSO solution of the imine (0.36 mmol in 5 ml DMSO) at 30 °C for 1 h at pH 8. Then particles were magnetically separated washed with 3 ml (3×1) methanol and again dispersed in 5 ml deionized water.

2.3. Characterization

The phase formation and crystallographic state of uncoated as well as functionalized magnetite particles were determined by an Expert Pro (Phillips) X-ray diffractometer using CoK_α. The particle size and microstructure were studied by transmission electron microscopy in a JEOL 2010F transmission electron microscope operating at 200 keV and the images were analyzed using image J software. Presence of surface functional groups was investigated by FTIR spectroscopy, Thermo Nicolet Nexux FTIR (model 870) and thermo gravimetric analysis (Pyris Diamond TG/DTA). Surface composition was investigated using X-ray photoelectron spectroscopy (VG Microtech) in ultra high vacuum with ALK_α and the data was analyzed using Origin 6.1

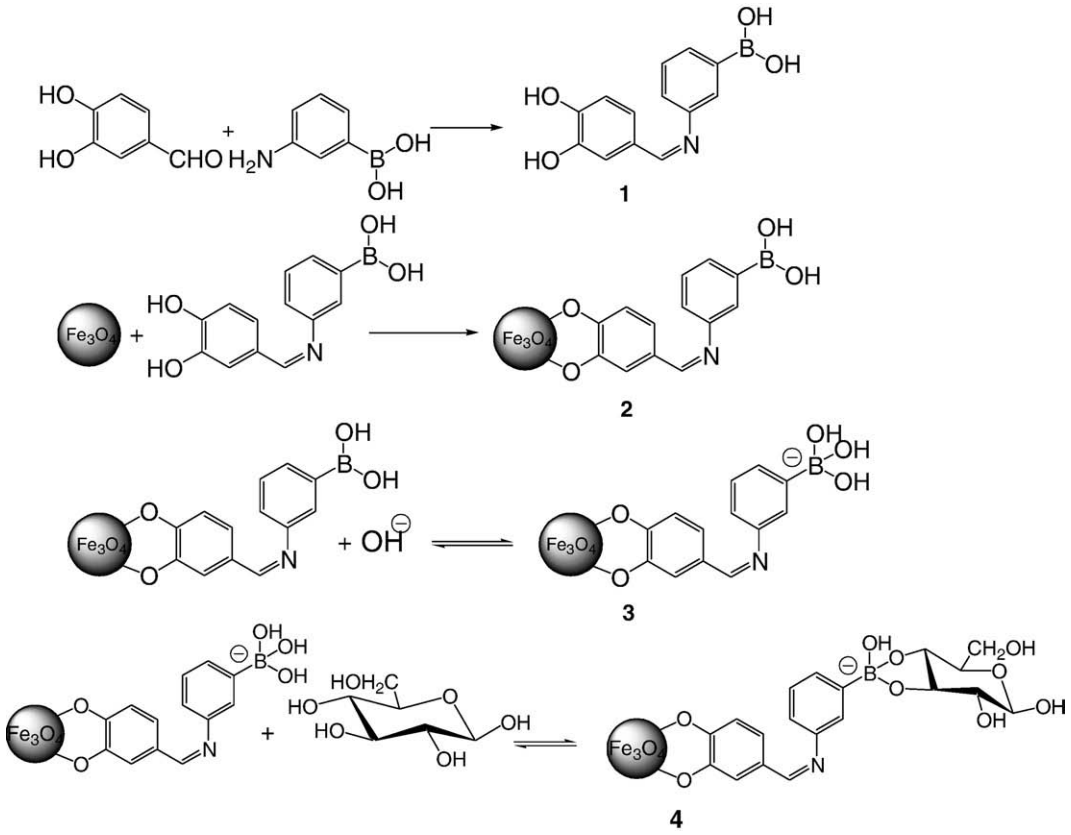

Scheme 1. Synthetic route and glucose binding mechanism of boronic acid functionalized magnetite nanoparticles.

Please cite this article as: S. Mohapatra, et al., Mater. Sci. Eng. (2009), doi:10.1016/j.msec.2009.05.017

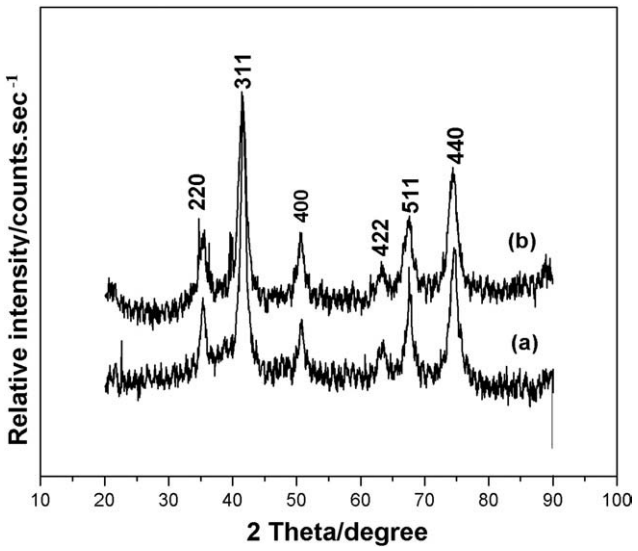

Fig. 1. X-ray diffractograms of a) as prepared iron oxide b) boronic acid functionalized iron oxide nanoparticles.

software. Magnetization measurement at room temperature was done by Lake Shore, Model-7410 magnetometer.

2.4. Estimation of sugar using boronic acid functionalized iron oxide nanoparticles

Prior to the binding process 500 mg of boronic acid-magnetite nanoparticles were dispersed in 40 ml millipore water. A certain volume of this suspension was taken and washed with millipore water (1 ml × 5). Then added 900 µl sugar solution (0.5 mg/ml) and 100 µl phosphate buffered saline and incubated for 4 h at room temperature with rocking. After the completion of adsorption period the particles were isolated using magnetic separator followed by washing with 2 × 1 ml millipore water and the supernatant was collected. The amount of bound sugar was determined from the concentrations of free sugars in the supernatant colorimetrically using 3, 5 dinitrosalicylic acid (DNS) test [26] and concentration of sugar was estimated from standard curve plotted taking different known concentrations of sugar in the *X*-axis and absorbance at 545 nm (the colour developed by DNS test) in *Y*-axis. This experiment was followed taking 25, 50, 75 and 100 µl of suspensions. The sugar binding was carried out at variable pH and temperature.

2.5. Adsorption of glycosylated hemoglobin

The preliminary investigation on adsorption of glycohemoglobin on synthesized boronic acid functionalized magnetic nanoparticles has been carried out. Red blood cells from 1 µl of anticoagulated (0.01% NH_4F treated) blood sample was taken and hemolysed with 0.01 N HCl and the volume was made up to 10 ml with phosphate buffered saline (PBS, pH 7.4). 900 µl of this hemolysed sample was incubated with certain quantity of nanoparticle suspension and 100 µl PBS at pH 8.5 at 4 °C for 3 h. The supernatant was taken out and absorption maximum was measured at 412 nm. In another tube the blood sample was taken without any nanoparticle in the same dilution and OD was taken at 412 nm. The same experiment was repeated for as prepared magnetite nanoparticles.

3. Results and discussion

Scheme 1 illustrates the synthetic route for the preparation of boronic acid functionalized iron oxide nanospheres. Fig. 1 shows the diffraction pattern of uncoated as well as boronic acid functionalized

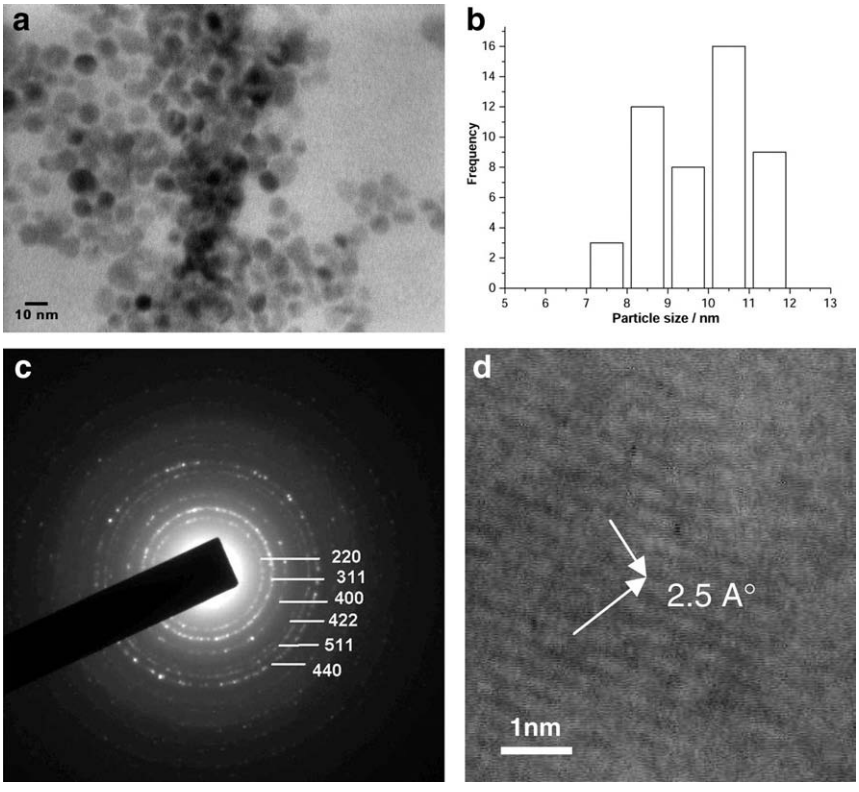

Fig. 2. a) TEM micrograph of boronic acid functionalized magnetite nanoparticles b) corresponding particle size distribution c) SAED pattern of Boronic acid functionalized magnetite particles d) HRTEM image of Boronic acid functionalized magnetite particles corresponding to lattice imaging of [311] plane.

Please cite this article as: S. Mohapatra, et al., Mater. Sci. Eng. (2009), doi:10.1016/j.msec.2009.05.017

iron oxide nanoparticles. For uncoated sample the *d*-values match with those for standard pattern of inverse spinel magnetite (Fe_3O_4) (JCPDS file no 82-1533). There is no phase change observed after surface functionalization. The peak positions didn't shift but showed a little broadening. The mean crystallite sizes were calculated taking into account broadening of each peak using Scherer's equation and were found to be 12 nm for as prepared magnetite particles and 8 nm for boronic acid functionalized magnetite particles. The crystallinity of both samples was calculated from the h/w ratio of the most intense [311] peak. It decreases from 0.3 to 0.23 after coating, which indicates relatively poor crystallinity at the interface after surface modification due to binding of enediol group of the imine on iron oxide surface. It is already established by Rajh et al. [27,28] through spectroscopic studies that the bidentate enediol ligands convert the under-coordinated Fe surface sites back to a bulk like lattice structure with an octahedral geometry for oxygen coordinated iron, which may result tight binding of the ligand to the iron oxide surface.

Fig. 2a shows TEM image of ultrafine boronic acid functionalized particles in PBS at pH 8. The boronic acid functionalized magnetite particles show remarkably well dispersed particles with narrow particles size distribution (Fig. 2b). The mean average particle size was found to be 10 ± 0.5 nm. The well dispersion of particles may be due to electric force of repulsion between boronate groups which prevents particle agglomeration. The selected area electron diffraction (SAED) of the synthesized boronic acid modified magnetic particles shows distinct rings which is characteristic of polycrystalline samples. The *d*-values were calculated from the formula

$$d = \frac{\lambda L}{R}$$

Where λ = Wavelength of electron wave
L Camera length
R Radius of diffraction ring

The *d*-values indexed in SAED pattern correlates with that of XRD pattern. The high resolution TEM image of boronic acid modified particles shows lattice imaging of [311] plane.

The transmission infrared spectra of both as prepared and boronic acid functionalized magnetite nanoparticles are shown in Fig. 3 along with the boronic acid imine. Band at low frequency region (1000–300 cm^{-1}) is due to the iron oxide skeleton. The Fe–O stretching vibration appears at 570 cm^{-1}, which is the typical characteristic of magnetite. The intensity of the band at 570 cm^{-1} is less in case of coated particles indicating the adsorption of boronic acid imine on the surface of the magnetite nanoparticle. O–H stretching vibration at about 3410 cm^{-1} and O–H deformation vibration at 1625 cm^{-1} in both uncoated and coated particles indicate that both have –OH rich surface. As compared to the uncoated particle boronic acid functionalized magnetite particles (Fig. 3c) shows bands between 1360 to 1060 cm^{-1} and 1032 to 730 cm^{-1} corresponding to in-plane and out of plane bending vibration of C–H bond respectively. Absorption at 3000 cm^{-1} corresponds to C–H stretching of aromatic ring. Band 1530 cm^{-1} corresponds to C=N stretching of the imine group. The comparison between FTIR spectra of uncoated and boronic acid coated magnetite nanoparticles gives evidence for chemical bonding of boronic acid imine on the magnetite surface which is further supported by XPS and thermal analysis.

XPS study under ultrahigh vacuum using AlK_α was used to follow the surface modification of iron oxides with boronic acid and the chemical composition of the surface (Fig. 4). Peaks at C1s region show that C atoms are involved in four different environments. Peak centered at 284.6 eV accounts for reference carbon and the aromatic carbons present in the benzene ring of the imine. The small component of C1s peaked at 283.2 is very close to that for C–B bond [29]. The contributions of 285.86 eV reveal the presence of C of C=N bond and the binding energy of 288.5 eV corresponds to C–O bond. This gives evidence for the presence of boronic acid imine (1) on the surface. O1s binding energy, which appears at 527.2 to 537.3 eV, can be nicely fitted into three peaks at 530.5, 531.5 and 532.08 eV. Peak at 530.5 corresponds to Fe–O and 531.5 eV corresponds to B–O bond. Peak centered at 532.05 eV is slightly greater than that of Si–O–Fe bond as reported by Woo et al. in connection with surface modification of Fe_2O_3 particles with a silane coupling agent [30]. Hence it can be attributed to O1s electrons present in Fe–O–C bond. N1s shows a single peak at 398.8 eV corresponding to C=N bond in accordance with the values reported by Dementjev et al. [31] and Bhattacharya et al. [32]. Fe2p electrons show binding energy at 710 and 725 eV in consistency with the values obtained for Fe_3O_4. The broad peak appeared at 184–194 eV corresponds to B1s binding energy. It can be deconvoluted into two peaks centered at 188.05 and 190.04 eV indicating boron present at two different environments. It might be due to the coordination of OH^- to boronic acid to form tetra-coordinated boron. The peak at 190.04 eV corresponds to phenyl boronic acid. Hence XPS data reveals that the boronic acid imine (1) has been coupled on magnetite surface through diol moiety.

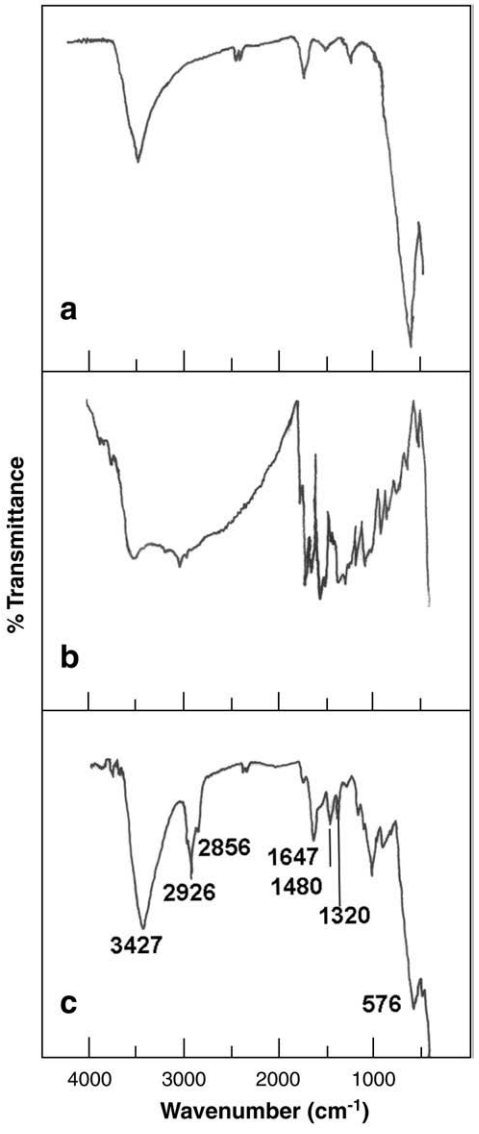

Fig. 3. Transmission FTIR spectra of a) as prepared magnetite b) synthesized boronic acid imine c) boronic acid functionalized magnetite nanoparticles.

Please cite this article as: S. Mohapatra, et al., Mater. Sci. Eng. (2009), doi:10.1016/j.msec.2009.05.017

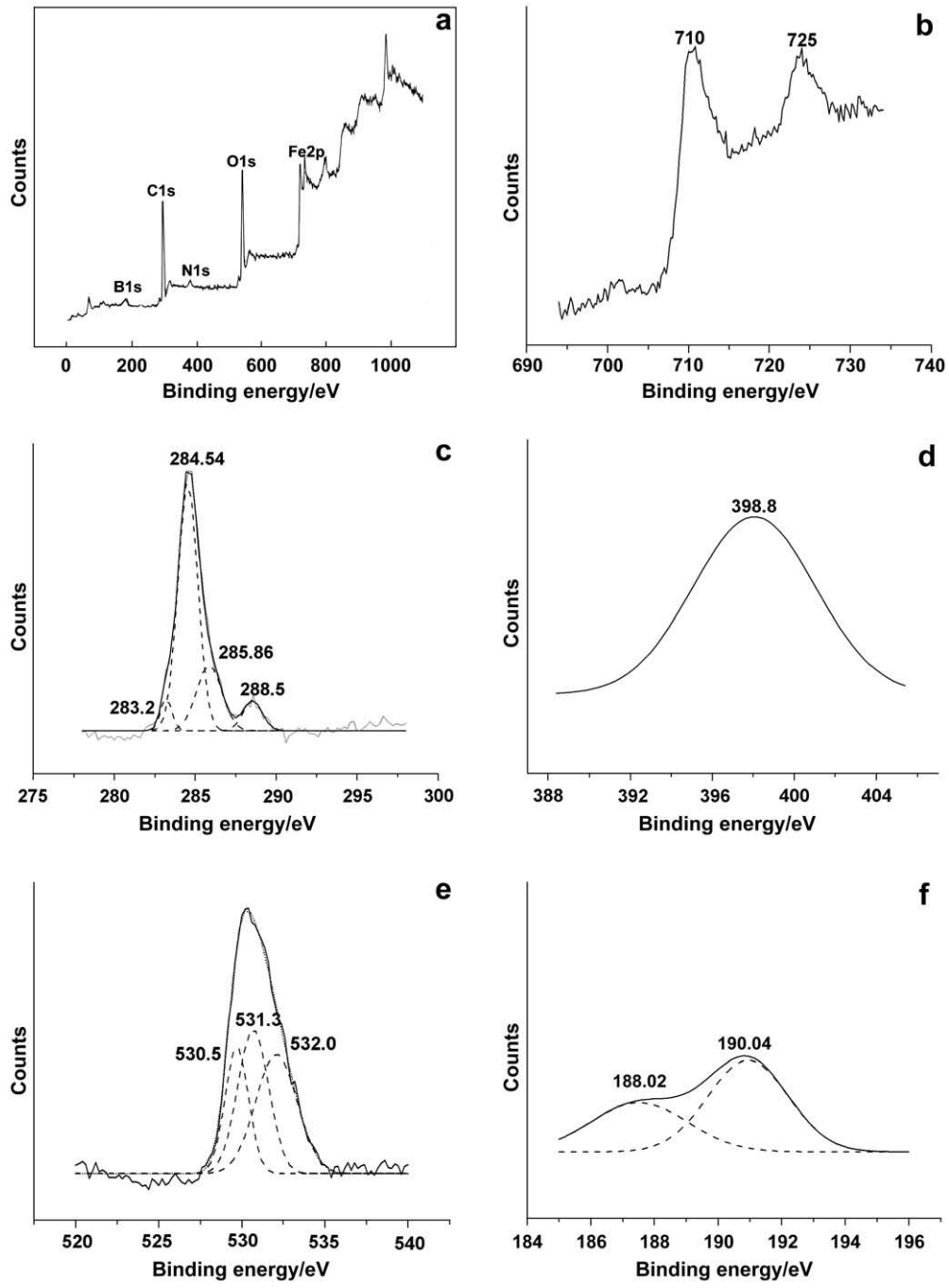

Fig. 4. XPS spectrum boronic acid functionalized magnetite particles using AlK_{α} source. a) Survey b) Fe2p c) C1s d) N1s e) O1s f) B1s.

The thermogravimetric analysis curves of the magnetite nanoparticles and boronic acid functionalized magnetite particles are shown in Fig. 5. The initial weight loss from the uncoated magnetite particles up to 200 °C is due to the loss of physically adsorbed water, surface hydroxyl groups while the loss at higher temperature may be attributed to the decomposition of amorphous iron hydroxides followed by formation of iron oxide [33]. Basing on the TG curve of the uncoated particle the initial weight loss in boronic acid functionalized particles is due to loss of physically adsorbed water and surface hydroxyl groups, while weight loss at higher temperature may be attributed to the evaporation and subsequent decomposition of the organic coating. In addition to this, in comparison to the uncoated magnetite the weight loss in boronic acid functionalized nanoparticle up to 200 °C is ~8% lower indicates the less number of hydroxyl groups or adsorbed water molecules on the surface. This result further gives information that boronic acid imine molecules are bonded onto magnetite surface through enediol group. The less number of hydroxyl groups is due to the reaction of surface hydroxyl and enediol groups followed by removal of water.

Fig. 6 shows magnetization curves of unmodified (a) and surface functionalized (b) magnetite nanoparticles. The magnetization curves of both uncoated magnetite and coated magnetite do not show any hysteresis opening and are completely reversible at room temperature. Coercivity and remanence were not observed indicating superparamagnetism in both samples. The least squares fit showed that the magnetization curves obeyed Langevin function. From M vs 1/H plot the saturation magnetization σ_s for uncoated magnetite is 64 emu/g which is much less than its bulk counter part. In addition to the

Please cite this article as: S. Mohapatra, et al., Mater. Sci. Eng. (2009), doi:10.1016/j.msec.2009.05.017

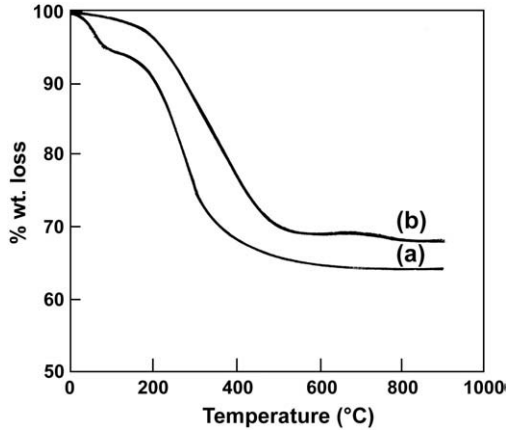

Fig. 5. Thermogram of a) uncoated magnetite b) boronic acid functionalized magnetite.

dilution effect from antiferromagnetic amorphous iron oxide and adsorbed water and hydroxyl groups this significant decrease in magnetization could be attributed to small particle size [34]. For boronic acid modified magnetite particles the magnetization obtained at same field is 52 emu/g. Besides detachment from magnetic coupling this small decrease in magnetization could be attributed to the spin pinning effect [35], which originates from Fe–O–C bond formed between surface Fe atoms and –OH group of the imine. The existence of Fe–O–C bond was also supported by FTIR and thermal analysis. Magnetic diameters (D_m) for both samples have been calculated from hysteresis loops, assuming log normal distribution according to TEM observation. D_m for as prepared uncoated and boronic acid modified magnetite particles were found to be 20.2 nm and 14.8 nm respectively. The good agreement between D_m and D_{xrd} particularly incase of modified samples indicates that the magnetic interaction between the particles has been prevented.

3.1. Sugar adsorption experiment

The sugar binding capacity of synthesized boronic acid modified nanoparticles was investigated taking dextrose sugar. The adsorption experiment was carried out in separate batches at 4, 25, 37 and 45 °C in phosphate buffer. The pH of the adsorption was varied using 0.1 HCl and 0.1 NaOH. The amount of dextrose sugar in the supernatant was quantified from 3, 5 dinitrosalicylic acid test (DNS). 3, 5 dinitrosalicylic acid gets reduced to 3-amino 5-nitrosalicylic acid by dextrose at alkaline pH which produces orange red colour (λ_{max} 540 nm). The calibration curve was prepared by taking known concentrations of

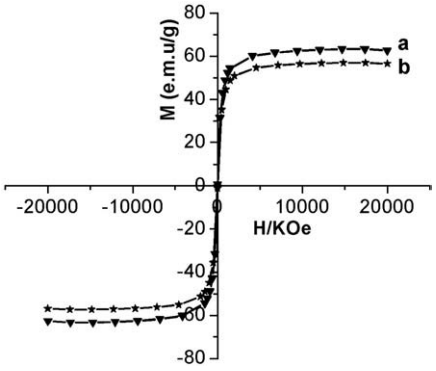

Fig. 6. Magnetization data of a) as prepared magnetite and b) boronic acid coated magnetite at room temperature.

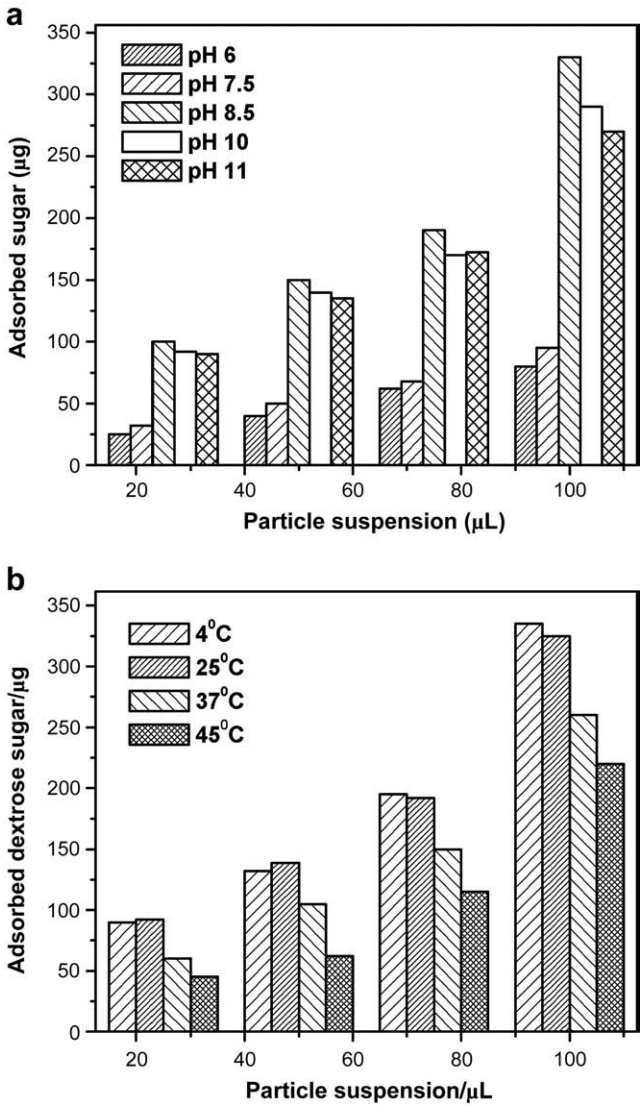

Fig. 7. a) Effect of pH on sugar adsorption on boronic acid functionalized magnetite nanoparticles. b) Effect of temperature on sugar adsorption on boronic acid functionalized magnetite nanoparticles.

sugar solution and measuring OD at 540 nm after reacting with DNS. Comparing the OD of supernatant with calibration curve, the quantity of sugar in the supernatant was estimated. Then deducting the amount of unbound sugar from total sugar concentration the quantity of adsorbed sugar was calculated.

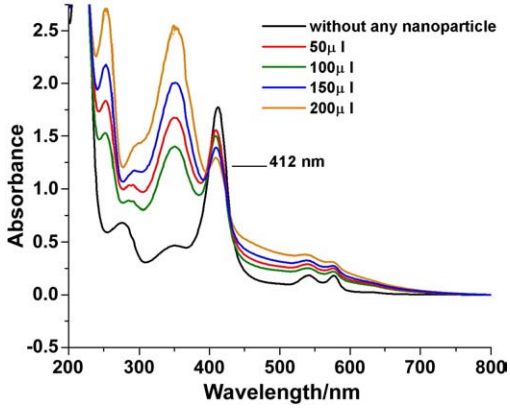

Fig. 8. Change in absorption maxima of the supernatant of blood with increase in nanoparticle suspension.

Please cite this article as: S. Mohapatra, et al., Mater. Sci. Eng. (2009), doi:10.1016/j.msec.2009.05.017

3.2. Effect of pH

Fig. 7a shows the effect of pH on sugar adsorption at 25 °C. It is observed that as the pH raises from 6 to 8.5 the adsorption increases and then deceases. As reported in literature the binding of boronic acid group to cis 1, 2 diol of sugar occurs in two steps. First boronic acid is transformed to tetrahedral anionic form [20] which subsequently binds with diol to form cyclic ester. pK_a value of phenyl boronic acid is 8.7–8.9 [36]. Based on this value most of the boronic acid will remain in trigonal form at pH equal to or less than 7, which does not react with diol group of sugar as described in literature [37]. Therefore low sugar adsorption was observed at pH 6 and 7. However at pH close to pK_a boronic acid is expected to exist in tetrahedral boronate form which facilitates the formation of cyclic boronate ester. Therefore higher adsorption was obtained at pH 8.5 or above. Shimomura et al. have calculated the pK_a value of immobilized phenyl boronic acid on magnetic support as 9.2 [19], slightly higher than free phenyl boronic acid and shown that the adsorption of adenosine was highest at pH 10–11. Our results don't tally with that reported by Shimomura et al. However, it is consistent with observations reported by Elmas et al. [16] for adsorption of β-NAD on thermosensitive N-isopropylacrylamide-vinylphenyl boronic acid copolymer latex particles. In our case the synthesized and the boronic acid modified magnetic nanoparticles have maximum sugar adsorption capacity of approximately 3.5 μg/μl at pH 8.5.

3.3. Effect of temperature

The effect of temperature on dextrose sugar adsorption has been presented in Fig. 7b. The pH of the experiment was fixed at 8.5. As seen in figure, with increase in temperature the sugar adsorption has been significantly affected at higher temperature. No remarkable difference was observed for 4 and 25 °C. However, at 37 and 45 °C the adsorption is reduced. This reduction might be due to agglomeration of magnetic nanoparticles at high temperature. This agglomeration causes reduction in surface area which ultimately causes decrease in adsorption capacity. Hence high temperature is formidable for performing adsorption experiments on these functionalized magnetic nanoparticles.

3.4. Adsorption of glycosylated hemoglobin

Glucose sticks to hemoglobin present in red blood cells to form “glycosylated hemoglobin” or “glycohemoglobin”, commonly known as HbA1C. The more glucose in the blood, the more haemoglobin HbA1C will be present in the blood. Measurement of HbA1C is one of the best ways to monitor sugar level in blood. Immobilized boronic acid based agarose column chromatography has been conventionally used to isolate and estimate HbA1C from blood [38]. To test the HbA1 binding capacity of synthesized boronic acid functionalized nanoparticles it was incubated with hemolysed blood samples. Fig. 8 shows the UV–Visible spectra of supernatant after the adsorption with variable amount of nanoparticles. It was observed that OD of the supernatant at 412 nm was decreased with increasing nanoparticle amount. But no such change was observed with as prepared magnetite nanoparticles. This decrease in hemoglobin content is due to adsorption of glycosylated hemoglobin on synthesized boronic acid functionalized magnetic nanoparticles. The quantitative adsorption and the effect of other parameters on adsorption of HBA1C are under further investigation.

4. Conclusion

Superparamagnetic magnetite nanoparticles of mean size 8 ± 1 nm with surface boronate ligands have been prepared. *m*-Aminophenyl boronic acid was successfully immobilized on magnetite surface through 3,4-dihydroxy benzaldehyde. FTIR shows the tight binding of enediol group on iron oxide surface forming Fe–O–C bond which is further supported by TEM and magnetization data. The sugar binding study shows that these beads have high sugar loading capacity at physiological pH. In conclusion, the material prepared in this work based on iron oxide particles could be a promising material for magnetic handling of sugars and sugar containing molecules at low concentration and offers new possibilities in biological applications.

Acknowledgement

Authors gratefully acknowledge CSIR, New Delhi for providing financial support for this work.

References

[1] D.S. Hage, Clinical Chemistry 5 (1999) 593.
[2] H.L. Weith, J.L. Weibers, P.T. Gilham, Biochemistry 9 (1970) 4397.
[3] M. Rosenberg, J.L. Weibers, P.T. Gilham, Biochemistry 11 (1972) 3623.
[4] J. Yoon, A.W. Czarnik, J. Am. Chem. Soc. 114 (1992) 5874.
[5] Y.C. Li, U. Pfüller, E.L. Larson, H. Jungvid, I.Y. Galaev, B. Mattiasson, J. Chromatogr. A 925 (2001) 115.
[6] T.D. James, K.R.A.S. Sandanayake, S. Shinkai, Nature 374 (1995) 345.
[7] T.D. James, K.R.A.S. Sandanayake, S. Shinkai, Angew. Chem., Int. Ed. Engl. 35 (1996) 1910.
[8] S. Striegler, Curr. Org. Chem. 7 (2003) 82.
[9] H. Schott, E. Rudloff, P. Schmidt, R. Roychoudhury, H. Kössel, Biochemistry 12 (1973) 932.
[10] M.F. Pougam, B.D. Smith, Tetrahedron. Lett. 34 (1993) 3723.
[11] L.K. Mohler, A.W. Czarnik, J. Am Chem. Soc. 115 (1993) 7037.
[12] K. Tsukagoshi, S. Shinkai, J. Org. Chem. 56 (1991) 4089.
[13] J. Yoon, A.W. Czarnik, J. Am. Chem. 114 (1992) 5874.
[14] P. Hazot, T. Delair, A. Elaissarï, J.P. Chapel, C. Pichot, Colloid Polym. Sci. 56 (2002) 6269.
[15] T. Koyama, K. Terauchi, J. Chromatogr. B 679 (1996) 31.
[16] B. Elmas, M.A. Onur, S. Senel, A. Tuncel, Colloids Surf. A: Physicochem. Eng. Asp. 232 (2004) 253.
[17] M. Uusi-Oukari, C. Ehnholm, M. Jauhiainen, J. Chromatogr. B 682 (1996) 233.
[18] H. Kitano, M. Kuwayama, N. Kanayama, K. Ohno, Langmuir 14 (1998) 165.
[19] M. Shimomura, T. Abe, Y. Sato, K. Oshima, T. Yamauchi, S. Miyauchi, Polymer 44 (2003) 3877.
[20] M. Shimomura, B. Ono, K. Oshima, S. Miyauchi, Polymer 47 (2006) 5785.
[21] A. Dayal, K. Loos, M. Noto, S.W. Chang, K.V.P. Spagnoli, M. Shafi, A. Ulman, M. Cowman, R.A. Gross, J. Am. Chem. Soc. 125 (2003) 1684.
[22] Z. Guo, Y. Sun, Biotechnol. Prog. 20 (2004) 500.
[23] S.H. Huang, M.H. Liao, D.H. Chen, Biotechnol. Prog. 19 (2003) 1095.
[24] S. Mohapatra, D. Pal, S.K. Ghosh, P. Pramanik, J. Nanosci. Nanotechnol. 7 (2007) 3193.
[25] J.M. Perez, T. O Loughin, F.J. Simeone, R. Weissleder, L. Josephson, J. Am. Chem. Soc. 124 (2002) 2856.
[26] J.B. Sumner, T. Vras, J. Biol. Chem. 47 (1921) 5.
[27] L.X. Chen, T. Liu, M.C. Thurnauer, R. Csencsits, T. Rajh, J. Phys. Chem. 106 (2002) 8539.
[28] T. Rajh, L.X. Chen, K. Lukas, T. Liu, M.C. Thurnauer, D.M. Tiede, J. Phys. Chem. B 106 (2002) 10543.
[29] H. Ling, J.D. Wu, J. Sun, W. Shi, Z.F. Ying, F.M. Li, Diamond Relat. Mater. 11 (2002) 1623.
[30] T. Woo, J.Y. Huh, D.E. Nikles, IEEE Trans. Magn. 37 (2001) 1634.
[31] A.P. Dementjev, A. de Graaf, M.C.M. van de Sanden, K.I. Maslakov, A.V. Naumkin, A. A. Serov, Diamond Relat. Mater. 9 (2000) 1904.
[32] S. Bhattacharya, C. Cardinaud, G. Turban, J. Appl. Phys. 83 (1998) 4491.
[33] F.S. Yen, W.C. Chen, Y.M. Yang, C.T. Hong, Nano Lett. 2 (2002) 245.
[34] B. Martinez, X. Obradors, L.I. Balcells, A. Rouanet, C. Monty, Phys. Rev. Lett. 80 (1998) 81.
[35] A.E. Berkowitz, J.A. Lahut, I.S. Jacobs, L.M. Levinson, D.W. Forester, Phys. Rev. Lett. 34 (1975) 594.
[36] K. Kataoka, H. Miyazaki, T. Okano, Y. Sakurai, Pharm. Res. 14 (1997) 289.
[37] E. Uguzdogan, E.B. Denkbas, A. Tuncel, Macromol. Biosci. 2 (2002) 214.
[38] F.A. Middle, A. Bannister, A.J. Bellingham, P.D.G. Dean, Biochem. J. 209 (1983) 771.

Please cite this article as: S. Mohapatra, et al., Mater. Sci. Eng. (2009), doi:10.1016/j.msec.2009.05.017